

## Characterization of creep deformation and rupture behaviour of P92 steel weldment at 600°C

**N.A. Alang**

Structural Material and Degradation Focus Group,  
Faculty of Mechanical Engineering, Universiti Malaysia Pahang  
26600 Pekan, Pahang, Malaysia,  
Email: [azuan@ump.edu.my](mailto:azuan@ump.edu.my)  
Phone: +6094246266; Fax: +6094246222

### ABSTRACT

P92 steel is a potential candidate for ultra-supercritical (USC) plant component. Thus, its suitability and performance for future service are still under investigation. Understanding the creep behaviour is essential to design the components that can sustain in service over a certain period. With the intention to investigate the creep deformation and rupture behaviour of P92 steel weldment, four cross-weld creep specimens were prepared and tested at 600°C at different stress levels. All specimens ruptured between 400 and 4,000 hours. Following the creep test, fractography examination was performed. P92 steel weldment exhibits clear primary, secondary and tertiary creep deformation stages. At long-term, the time portion for primary deformation as compared to rupture time reduces, however, secondary stage is observed to dominate. Deformation and rupture data obeys the power law relation which indicates the material deforms at a higher rate and rupture earlier as the stress increases. Ductility of P92 steel weldment reduces as the stress decreases. A strong correlation between minimum creep strain rate and time to rupture is observed when the data is fitted using original Monkman-Grant (MG) and Modified Monkman-Grant (MMG) relations. Examination of fracture surface reveals that at high stress, transgranular-type of fracture is dominant. As creep time increases, a mixture between the intergranular and transgranular fracture is evidence.

**Keywords:** Creep; deformation; Monkman-Grant; P92 steel weldment; rupture.

### INTRODUCTION

In power generation plant, components are subject to creep damage which developed during long-term high temperature exposure under static or dead load. Microscopic examination on the ex-service components reveals that damage in terms of voids and micro-cracks distribute mainly at the grain boundaries [1,2]. This type of damage causes the material to fracture in a brittle manner associated with reduced creep strength [3]. The development of voids and micro-cracks in creep environment are complex, therefore is still not fully understand. One of the currents practises delaying the progression of damage is simply by reducing service temperature and pressure. However, this leads to the higher emission of carbon dioxide (CO<sub>2</sub>) to the atmosphere and reduces the efficiency of the power plant in generating the electricity.

In line with the intention to develop the power plant with higher thermal efficiency, having the material that can sustain at high operating temperature and pressure without failure is vital. Instead of relatively cheaper compared to the nickel-based alloy which is ten times costlier [4], P92 steel exhibits fairly high creep strength and ductility, therefore, becomes a potential candidate for such plant. In fact, P92 possess acceptable resistance to the oxidation which makes the material suitable for the long-term application. In recent years, numbers of creep rupture test have been performed on

P92 steel base metal [5-7]. The test does not only help to understand the creep behaviour, but it is also essential when deriving the constitutive creep model which is the requirement for predictive modelling. As the creep behaviour of weld metal is different from base metal particularly at long-term where type IV cracking controlled the failure [8] and also responsible for the drop in creep strength and ductility, having sufficient creep data for weldment is also important to further investigate the material performance.

Experimentally, creep rupture life of welded power plant components can be determined by conducting long-term creep rupture testing. The experiment parameter is designed so that the material will experience as real service condition. However, such a long-term test is very costly, time-consuming and impractical. As an alternative, attempted has been made to predict the long-term creep behaviour based on the short-term creep test data [9-11]. At short-term, dislocation or power law creep is dominant while at long-term diffusion creep will take over. As a result, the changes in slopes of creep deformation and rupture curves have been observed [5].

Since the weld joint is inevitable and the fact that the available creep data for P92 weldment is very limited, the study is focused on this material. Creep deformation and rupture behaviour at temperature,  $T = 600^\circ\text{C}$  which is the typical operating of the power plant is systematically investigated and characterized. Upon the test, fractography of the crept specimen is examined to investigate the influence of stress and time on fracture mode.

### MATHEMATICAL FRAMEWORK

Numbers of empirical-based models have been developed which describes the dependence of rupture life on stress and temperature. Two common models that available in the literature are Monkman-Grant (MG) rule [12] and its modified form known as Modified Monkman-Grant (MMG) relation [13]. Mathematically, the MG relationship can be expressed as:

$$(\dot{\epsilon}_m)^{\beta'} \cdot t_r = C' \quad (1)$$

where the  $\dot{\epsilon}_m$  is the minimum creep strain rate,  $t_r$  is the rupture time,  $\beta'$  and  $C'$  are constants. Milicka and Dobes [13] noted that the scatter of the experimental data of Eqn. (1) can be reduced when modifying the MG relation by incorporating the creep rupture strain. The modified-MG relation can be written as:

$$\frac{\dot{\epsilon}_m^{\beta''} \times t_r}{\epsilon_f} = C'' \quad (2)$$

where  $\epsilon_f$  is the strain at rupture and,  $\beta''$  and  $C''$  are constants. To establish the abovementioned relation, sufficient number of creep data is required. Specifically for P92 steel, creep data for parent material is well reported in literature [14-16] and material database [17], however, very limited for weld metal. The limitation is probably due to the priority is given to parent material during the earlier work on data collection and also due to data confidentiality. To deal with the real component with complex stress state, Finite Element (FE) damage-based modelling may be an option. The method, however, required reliable creep constitutive and damage model to perform the prediction. One of the commons yet simple in form stress-strain relations is based on Norton power law [18]:

$$\dot{\epsilon}_m = A\sigma^n \quad (3)$$

where,  $A$  and  $n$  are the minimum or steady-state power-law constants. In order to account all three creep deformation stages, the average creep strain rate,  $\dot{\epsilon}_A$  is proposed and can be written using power law relationship as:

$$\dot{\epsilon}_A = A_A \sigma^{n_A} \tag{4}$$

where  $A_A$  and  $n_A$  are the average power-law constants. The  $\dot{\epsilon}_A$  at particular stress level,  $\sigma$  can be calculated using:

$$(\dot{\epsilon}_A)_\sigma = \left( \frac{\dot{\epsilon}_f}{t_r} \right)_\sigma \tag{5}$$

Similar form power law representation as for creep deformation can be applied to relate the rupture time to the applied stress and is expressed as:

$$t_r = M \sigma^{-v} \tag{6}$$

where  $M$  and  $v$  are coefficient and stress exponent of creep rupture relation.

### EXPERIMENTAL DETAILS AND MATERIALS

Spectrometric analysis was carried out to determine the chemical composition of the material. A sample of 20 mm x 20 mm was extracted from the material block, grinded and polished before being examined using spectrometry machine. The average reading of weight percentage of each element that has been taken from five different locations was calculated. The summary of chemical composition is shown in Table 1. The microstructure of the P92 steel was observed under optical microscope after mechanical grinding and polishing. The former process was done using grit papers (#600, #800, #1200 and #2500) whereas the later using diamond suspension liquid. Following the polishing, the sample was swabbed using a Vilella’s reagent, a mixture of 1g of acid picric + 5mL of hydrochloric acid (HCL) + 100mL of ethanol. The sample then was left for 15-20s before being cleaned under tap water. The microstructure of P92 weldment with 500X magnification is shown in Figure 1.

Table 1. Chemical composition of P92 steel (% wt).

Comp (% wt)	Cr	Mo	V	Mn	C	Nb	W	Si	Ni	S	P
P92 – PM	9.78	0.52	0.20	0.39	0.13	0.031	1.38	0.13	0.19	<0.005	<0.003
P92 – Weld	9.37	0.54	0.23	0.61	0.12	0.016	1.36	0.26	0.60	<0.005	<0.003

Under optical microscopy, P92 steel shows tempered-martensite microstructures. The martensitic lath structure and prior austenitic grain boundaries (PAGB) were visibly exposed. The distribution of the precipitates in the materials, however, is not clearly seen. For direct comparison between each region, some of the grain boundaries were drawn (shown as dashed lines) except for weld material (WM), as the grains not clearly exposed. It is found that the region that close to base material/heat affected zone (BM/HAZ) region or fine grain HAZ shows smaller grain sizes compared to the one in WM/HAZ region or coarse grain HAZ perhaps due to the thermal weld cycle. The distinction between grain sizes confirmed that mechanical heterogeneity existed in the region and may influence the overall creep behaviour.

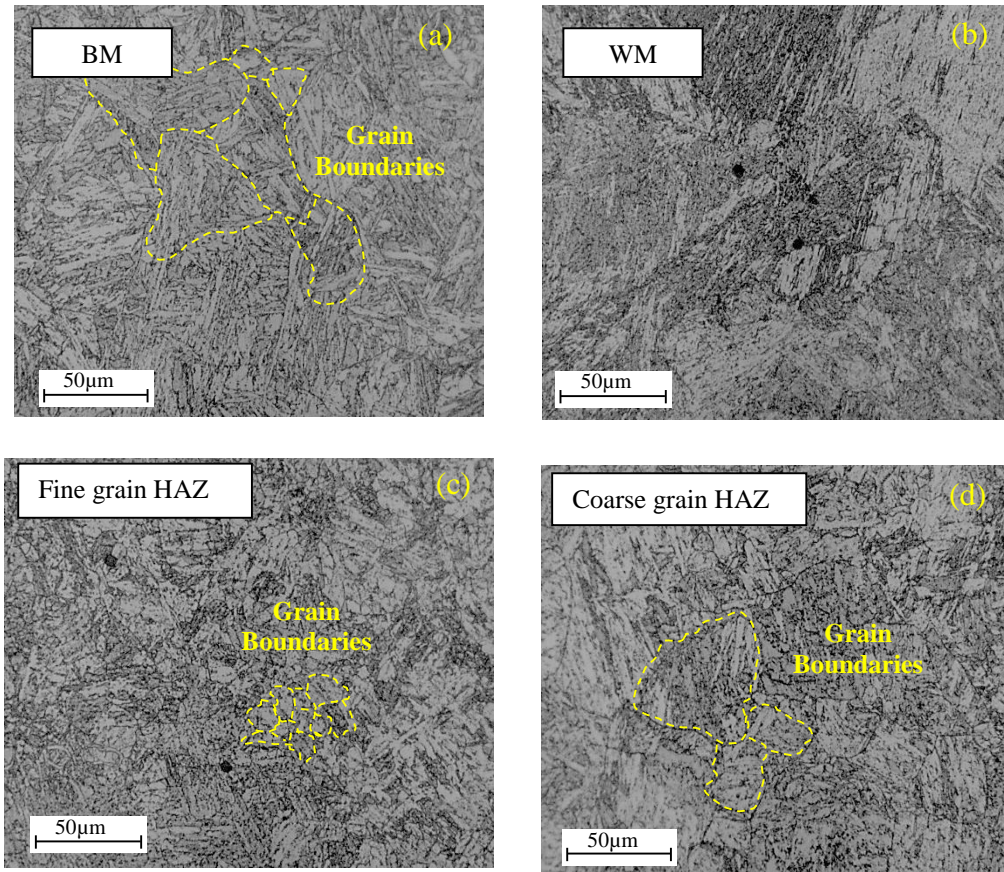


Figure 1. Optical micrograph of P92 weldment with magnification of 500X (a) BM, (b) WM, (c) fine grain HAZ and (d) coarse grain HAZ.

### Creep Rupture Test

Figure 2 shows the experimental setup and detail dimension of the specimen. Four P92 cross-welds (XW) uniaxial creep specimens were prepared and tested. The test was carried out at the stress range between 155 MPa and 180 MPa. All specimens were tested at the temperature of 600°C. During the test, the creep strain,  $\epsilon_c$  reading as a function of time,  $t$  is recorded. The test matrix which includes the specimen ID, stress level and temperature are shown in Table 2.

The creep rupture test was carried out according to the suggested test procedure ASTM E139-11 [19]. A dead-load creep machine was used to carry out the tests, which had a lever load ratio of 10:1. The specimen was held between two Nimonic holders inside the furnace. The rectangular-shape electric furnace was used to provide the high temperature environment around the specimen. The thermocouples were embedded in the furnace wall at three distinct locations: top, middle and bottom zones so that the heat in each zone could be slightly adjusted to obtain uniform temperature inside the furnace. However, it was found that the temperature measured by the thermocouples that implanted in the furnace was slightly different from the specimen's temperature. Therefore, two K-type thermocouple wires were locally attached to the specimen's surface within the gauge region to directly measure and monitor the temperature during the tests. The temperature was monitored so that they were within  $\pm 2^\circ\text{C}$  throughout the test. The readings from these two thermocouples are assumed to represent the overall temperature of the specimens in the gauge length region. The specimens were soaked for at least 24 hours to obtain stable high-temperature environment before the load was applied.

The elongation of the material in the longitudinal direction was measured using linear variable differential transformer (LVDT) that was centrally clamped between two aluminium plates. Prior to testing, the LVDT was calibrated and the calibration curve was obtained (voltage vs. displacement). During the load up, the voltage reading from the LVDT was continuously recorded in the data logger for every 5s whereas during creep (after load up) the recording time was increased to 300s. The elongation of the material was determined by converting the voltage output from the LVDT using the calibration curve that had been obtained earlier. The elongation of the specimen was monitored and the test was stopped when the specimen is broken.

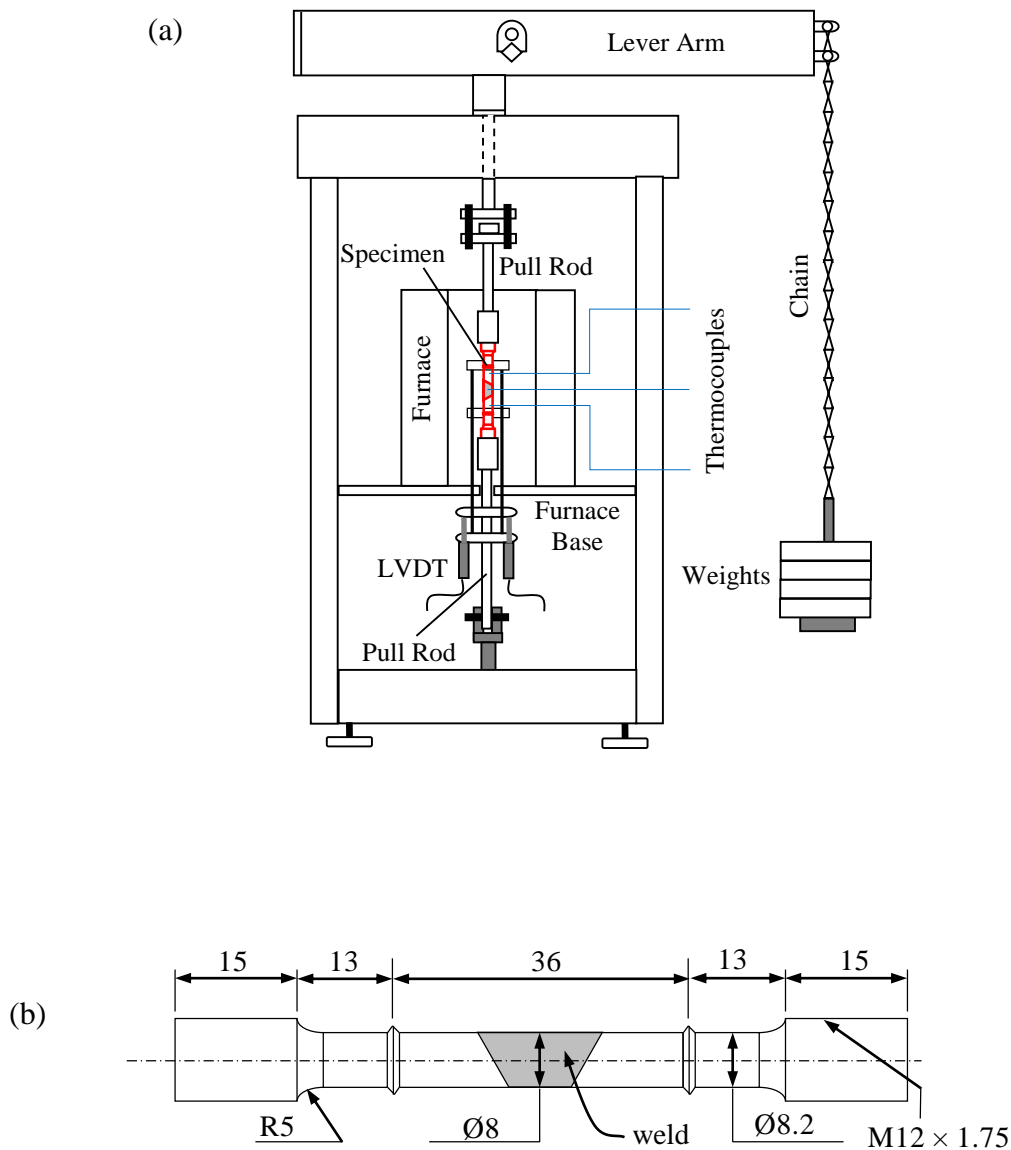


Figure 2. (a) Experimental setup and (b) detail dimension of the XW creep specimen.

Table 2. Creep rupture test matrix on uniaxial XW specimen.

Material	Specimen ID.	Stress (MPa)	Temp. (°C)
P92	XW_01	155	600
	XW_02	160	
	XW_03	170	
	XW_04	180	

## RESULTS AND DISCUSSION

### Creep Curve

The overall creep deformation as well as the creep strain rate against time are plotted and shown in Figure 3 and Figure 4. In general, all specimens obey the classical creep deformation theory which consists of three distinct stages: strain hardening (primary creep), steady state (secondary creep) and accelerated (tertiary creep). In the primary stage, the creep strain decreases over the time and the phenomenon called “strain hardening” is observed. The secondary or steady-state region is clearly observed before the creep strain starts to accelerate in the tertiary stage. At high stress, the secondary or steady state deformation is relatively shorter, however, it continues to increase and dominant as the stress decreases.

Within the test stress range, the tertiary deformation is found to begin after the creep strain accumulated between 2% and 3%. The failure strain which is quantified in terms of MG strain, elongation at rupture and Reduction of Area (ROA) show slight reduction in values as the stress decreases. At 180 MPa, the failure strain (elongation) of cross-weld (XW) specimen is approximately 13%. The value is relatively low with shorter creep lives compared to the parent material (PM) which usually ruptured at around 18% [14]. The behaviour may cause by the increase in constraint due to the creep damage development especially in the weld material (WM) and heat-affected zone (HAZ) regions.

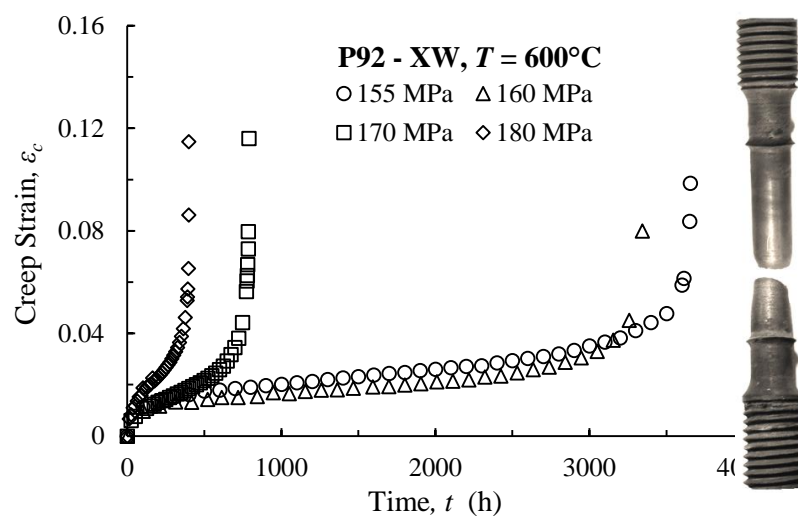


Figure 3. Creep strain curve for P92-XW.

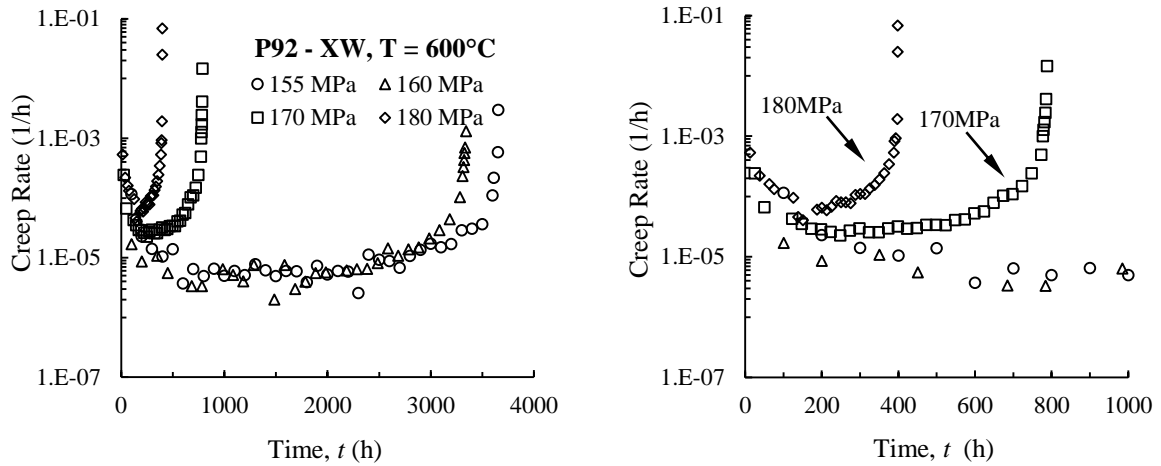


Figure 4. Evolution of creep strain for P92-XW (a) all stress levels and (b) close-up at  $0 < t < 1000$  hours.

The time fraction of each stage at different stress level is shown in Figure 5. The material spends largest portion of the life in steady state stage. The fraction for the primary stage is relatively small and even shorter as the stress decreases. Clearly, the secondary creep increases as the stress decreases. At 180 MPa, secondary stage takes around 40% of the total life and the value increases to 58% at 155 MPa. Apparently, the secondary creep is dominant in long-term times. The tertiary creep generally increases as the stress decreases; the exception is 155 MPa where the tertiary creep stage is the shortest compared to other stress levels. The heterogeneity of material properties of each material region of XW specimen may contribute to the inconsistency of the results.

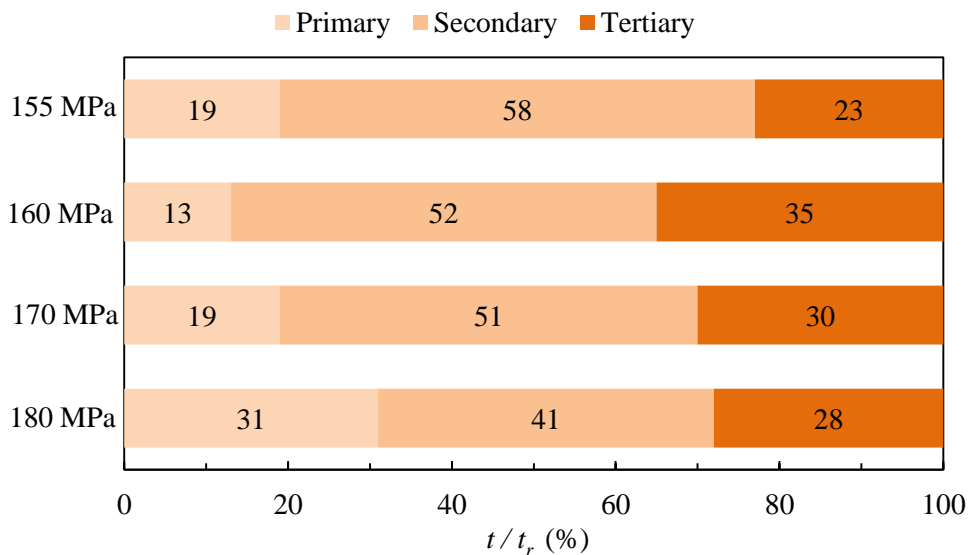


Figure 5. Relative time fraction for each creep stage for P92-XW.

**Creep Deformation and Rupture Behaviour**

Figure 6 shows the variation of creep strain rate,  $\dot{\epsilon}_c$  and rupture time,  $t_r$  against stress,  $\sigma$ . Noted that logarithmic scale is used for better representation of the data. The creep coefficient, ( $n$  and  $\nu$ ) and stress exponent, ( $A$  and  $M$ ) are both determined by plotting the linear regression curve of the experimental data. In Figure 6a, the solid line represents best fit curve for minimum creep strain rate data while the dashed line represents for average strain rate data. In general, the  $\dot{\epsilon}_c$  increases as the stress increases while the  $t_r$  increases as stress decreases. It is found that the creep strain rate and rupture data obeyed the power law relation (Eqn. (3) and Eqn. (6)) however, no changes in stress exponents (slope) were found in both Figure 6a and b within the investigated stress range. This reflects to a similar fracture mechanism of dislocation or power law dominant creep for all tested specimens.

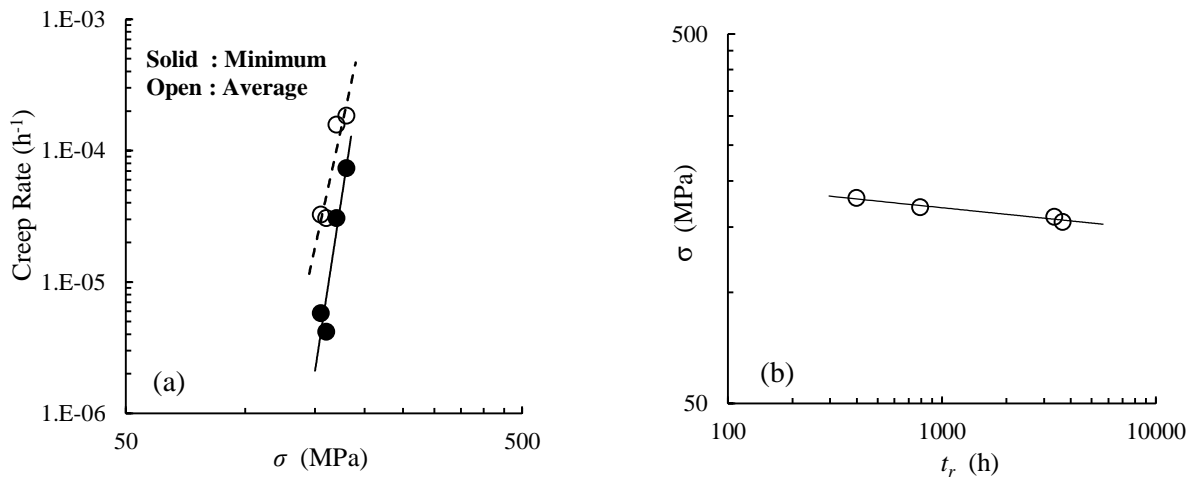


Figure 6. (a) Creep strain rate against stress and (b) stress against rupture time.

At long-term creep, a significant drop in creep strength of Grade 92 weldment has been observed [20]. Examination of the fracture surface reveals that substantial number of creep cavities particularly at HAZ region randomly distributed and linked together over time which finally causes type IV cracking. Consequently, the long-term creep data shifts away from short-term data trend. Thus, the overall data can be correlated well using two-slope Norton power law relation. In contrast, the data obtained in the current study do not show a similar trend. Examination of fracture surface shows that all specimens fracture at weld material which could be attributed to the lower creep ductility of weld material than that the base [3]. The total testing time is relatively shorter, therefore insufficient for the cavities to grow. As a result, no clear evidence that shows type IV governs the fracture is observed. Table 3 summarizes the value of power law constant, stress exponent and the coefficient for P92 weldment.

Table 3. Power law constant, stress exponent and coefficient for P92 weldment.

$T$ (°C)	$A$	$A_A$	$n$	$n_A$	$M$	$\nu$
600	$4.77 \times 10^{-49}$	$2.86 \times 10^{-35}$	19.6	13.7	$1.34 \times 10^{39}$	16.2

The rupture life-creep rate Monkman-Grant and its modified form relationship based on Eqn. (1) and (2) is presented in Figure 7. Similar to Figure 6, the logarithmic scale is used for both  $x$  and  $y$ -axes. For most steels, the  $\beta'$  and  $\beta''$  values have been reported close to unity [12], however, for the investigated material the values are 0.8 and 0.88, respectively. By using MG relation, the time to rupture can be estimated once the minimum creep strain rate is established. Therefore, the complete

rupture test (until the specimen broken) is not required. However, under multiaxial stress state, such as the case for the notched bar, determining the minimum creep strain rate is not straightforward, hence gives the shortcoming of using the MG relation.

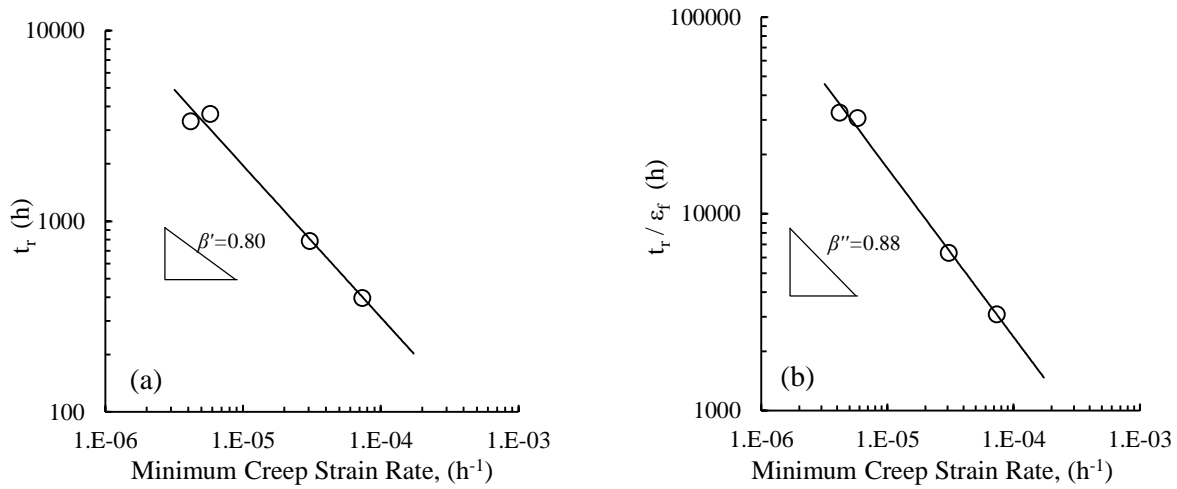


Figure 7. (a) Monkman-Grant relation and (b) Modified Monkman-Grant relation.

In 1952, Larson and Miller [21] proposed the relationship between stress, rupture time and temperature. Mathematically the relation can be written as follows:

$$LMP = (C + \log t_r) T \tag{7}$$

where LMP is the Larson-Miller parameter,  $C$  is the Larson-Miller constant and  $T$  is the temperature in Kelvin and  $t_r$  is the rupture time. Figure 8 shows the stress against LMP for P92 weldment at two different temperatures. Note that the rupture data at 650°C that is used to calculate the LMP is taken from [8]. Using the parameter,  $C=36.0$ , all the data can be fit by a single curve regardless of the temperature. The advantage of using LMP plot is that the rupture life at a particular stress level can be estimated easily based on the LMP value. Once the rupture data at one temperature is established, the prediction for other temperatures is also possible. For example, at 150 MPa, the corresponding LMP value is 34.6. Applying Eqn. (7), the rupture life at the temperature of 600°C and 650°C are 4300 h and 30.7 h, respectively.

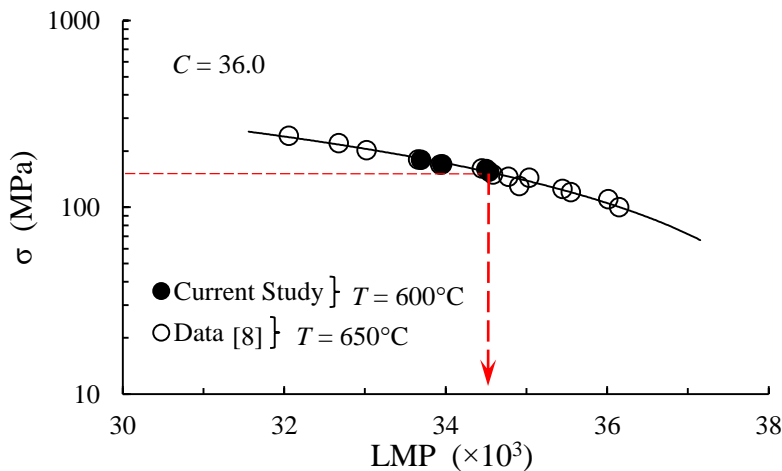


Figure 8. Stress against LMP for P92 weldment.

Figure 9 compares the reduction of area, ROA between the samples which is ruptured under different level of stress. In the case of high stress, significant necking is observed compared to the sample with lower stress. Further examination of the fracture surface of the specimen with  $\sigma = 180$  MPa revealed that a number of characteristic ductile dimples are dominant. The ductility (in term of reduction of area, ROA) reduces as the applied stress decreases, indicating the transition of fracture mode from ductile to brittle. A similar trend is also observed for Grade 91 steel at 650°C [22]. As the stress decreases to 160 MPa, the intergranular cracking is evident (Figure 9), but the ductile dimples are still dominant.

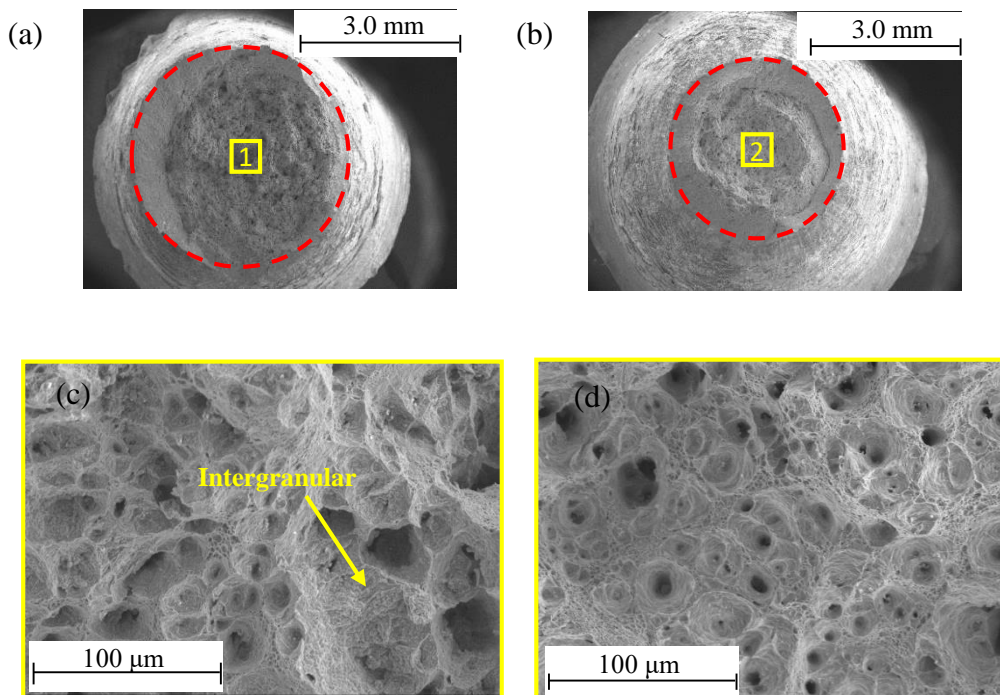


Figure 9. Fracture surface of P92-XW plain specimens (a) 160 MPa, (b) 180 MPa (c) close-up at point 1 and (d) close-up at point 2.

## CONCLUSIONS

Creep deformation and rupture behaviour of P92 steel weldment at 600°C were investigated. The following conclusions are reached:

1. P92 weldment showed clear primary, secondary and tertiary creep deformation stages. Both creep deformation and rupture data obeys the power law relation.
2. The minimum creep strain rate and rupture data is well correlated using MG and MMG relations with the slope  $\beta' = 0.8$  and  $\beta'' = 0.88$ , respectively. Using established correlation, extrapolation to longer time to predict long-term failure is possible. Employing a constant  $C$  of 36.0 (Eqn. (7)), a strong relationship between rupture data and LMP is obtained.
3. At the stress range of 155 MPa to 180 MPa, transgranular-type mode of fracture is dominant. Intergranular cracking is evidence at low stress, however, the area where this cracking mode occurred is small and insignificant.
4. Creep ductility of P92 steel weldment reduces as the stress decreases. The reduction in ductility at low stress could be attributed to the development of creep cavities and local constraint.

## ACKNOWLEDGEMENTS

The authors would like to thank to the Imperial College London and Universiti Malaysia Pahang for laboratory facilities and financial assistance, respectively.

## REFERENCES

- [1] Lillo T, Cole J, Frary M, Schlegel S. Influence of grain boundary character on creep void formation in Alloy 617. *Metallurgical and Materials Transaction A*. 2009;40:2803.
- [2] Ankit K, Prasad N. Simulation of creep cavity growth in Inconel 718 alloy. *Materials Science and Engineering: A*. 2011;528(12):4209-4216.
- [3] Alang NA, Nikbin K. An analytical and numerical approach to multiscale ductility constraint based model to predict uniaxial/multi-axial creep rupture and cracking rates. *International Journal of Mechanical Sciences*. 2018;135:342-352.
- [4] Igwemezie VC, Ugwuegbu CC, Mark U. Physical metallurgy of modern creep-resistant steel for steam power plants: Microstructure and Phase Transformations. *Journal of Metallurgy*. 2016;19.
- [5] Samuel EI, Choudhary BK, Palaparti DP, Mathew MD. Creep deformation and rupture behaviour of P92 steel at 923K. *Procedia Engineering*. 2013;55:64-69.
- [6] Petry C, Lindet G. Modelling creep behaviour and failure of 9Cr-0.5Mo-1.8W-VNb steel. *International Journal of Pressure Vessels and Piping*. 2009;86:486-494.
- [7] Lee JS, Armaki HG, Maruyama K, Muraki T, Asahi H. Causes of breakdown of creep strength in 9Cr-1.8W-0.5Mo-VNb steel. *Materials Science and Engineering A*. 2006;428:270-275.
- [8] Xue W, Pan QG, Ren YY, Wei S, Zeng HQ, Hong L. Microstructure and type IV cracking behaviour of HAZ in P92 steel weldment. *Materials Science and Engineering A*. 2012;552:493-501.
- [9] Brown SGR, Evan RW, Wilshire B. A comparison of extrapolation techniques for long-term creep strain and creep life prediction based on equations designed to represent creep curve shape. *International Journal of Pressure Vessels and Piping*. 1986;24:251-268.
- [10] Kim WG, Park JY, Jang J, Choudhary BK, Kim SJ, Kim YW, Jeong YH. Methodologies for long-term creep life extrapolation of Gr. 91 steel. In: Marquis F. (eds). *Proceeding of the 8<sup>th</sup> Pacific Rim International Congress on Advanced Materials and Processing*. Springer, Cham.
- [11] Wilshire B, Scharning PJ. Rationalization and extrapolation of creep and creep fracture data for Grade 91 steel. *Materials at High Temperature*. 2014;25:55-65.
- [12] Monkman FC, Grant NJ. An empirical relationship between rupture life and minimum creep rate in creep-rupture tests. *Proc. ASTM*. 1956;56:593-620.
- [13] Dobes F, Milicka K. On the Monkman-Grant relation for small punch test data. *Mater. Sci. Eng. A*. 2002;336(1-2): 245-248.
- [14] Panait CG. Metallurgical evolution and creep strength of 9-12%Cr heat resistant steels at 600°C and 650°C. PhD Theses, L'Ecole Nationale Supérieure Des Mines de Paris. 2010.
- [15] Wasmer K. Prediction of creep crack growth in a range of steels. PhD Theses, Imperial College London, 2003.
- [16] Rantala J. Creep test results for A617 and P92 – Uniaxial and notched bar, MACPLUS WP6, VTT, 2014.
- [17] NIMS. 9Cr-0.5Mo-1.8W-VNb (tube and pipe). Creep datasheet No. 48A, National Institute of Materials Science, Japan, 2012.
- [18] Norton FH. *The creep of steels at high temperatures*. McGraw-Hill, New York, 1929.

- [19] ASTM E139. Standard Test Methods, Conducting creep, creep-rupture and stress-rupture tests of metallic materials, American Standard Testing Materials, 2011.
- [20] Sakthivel T, Vasudevan M, Laha K, Parameswaran P, Chandravathi KS, Selvi SP, Maduraimuthu V, Mathew MD. Creep rupture behaviour of 9Cr-1,8W-0.5Mo-VNb (ASME Grade 92) ferritic steel weld joint. *Materials Science and Engineering A*. 2014;591:111-120.
- [21] Larson FR, Miller J. A time-temperature relationship for rupture and creep stresses. *Trans. ASME*. 1952;74:765-771.
- [22] Cipolla L. Microstructural evolution during long-term creep tests of 9%Cr steel grades. *Eight International Conference on Creep and Fatigue at Elevated Temperatures*. Texas, USA. 2007.